Electronic Supplementary Material (ESI) for Physical Chemistry Chemical Physics.

Supporting Information: Impact of the Sr content on the redox thermodynamics and kinetics of $Ca_{1-x}Sr_xMnO_{3-\delta}$ for tailored properties

1 X-ray diffraction

The structure of the perovskite for the thermodynamic analysis was studied with powder X-ray diffraction (XRD) using a *D8-Advance (A25)* instrument from *Bruker* with a copper anode and a *Lynxe-EyeXET-Detector* (fig.1).

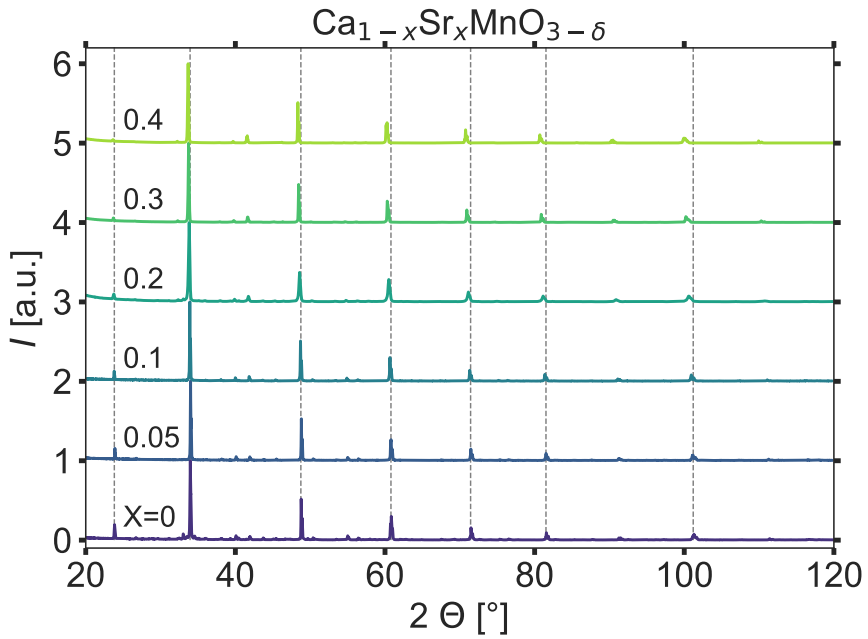

Figure 1 XRD-patterns of the perovskites prepared for the thermodynamic analysis. This patter was measured with a copper anode. The vertical lines indicate the main peaks of the structure with which this pattern was identified.

The structure of the perovskite for the kinetic analysis was studied with powder X-

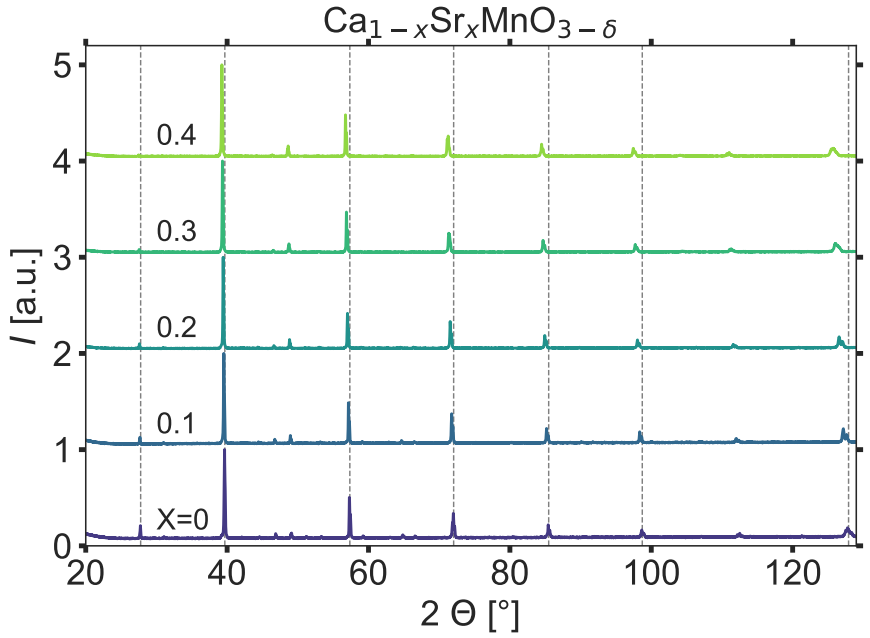

Figure 2 XRD-patterns of the perovskites prepared for the kinetic analysis. This patter was measured with a cobalt anode. The vertical lines indicate the main peaks of the structure with which this pattern was identified and which is the same as in fig. 1.

ray diffraction (XRD) using a *D8-Advance (A25)* instrument from *Bruker* with a cobalt anode and a *Lynxe-EyeXET-Detector* (fig.2).

The figures 1 and 2 show that the samples used for the thermodynamic as well as for the kinetic measurement have an orthorhombic structure with space group *Pnma* (PDF 01-074-8781 from the database *PDF 2 - Release 2019 RDB* of the *International Center for Diffraction Data (ICCD)*) without major side phases. The vertical lines indicate the main peak positions of this phase. The shift of the peaks to lower 2Θ-values are caused by the expansion of the lattice parameters due to the increased ionic radius of Sr compared to Ca[1]. The prepared samples are independent of the synthesis route.

2 Thermogravimetric scans

The thermodynamic analysis of the samples $Ca_{1-x}Sr_xMnO_{3-\delta}$ was performed in a *STA 449 F3 Jupiter Netzsch* thermobalance as described more detailed in the publication. To cover a wide range of oxygen partial pressure, each sample was first measured with a mixing of Ar, N_2 and O_2 (p_{O_2} = 0.83 bar to 0.1 bar) and then Ar, N_2 and synthetic air (p_{O_2} = 0.01 bar to 1×10^{-4} bar). These two measurements for $Ca_{0.9}Sr_{0.1}MnO_{3-\delta}$ as

an example are shown in fig. 3 and 4. In the displayed graphs, a blank measurement subtraction as well as a linear drift correction was already applied. As for the lowest oxygen partial pressure the kinetics were slowly (fig. 4), the sample was first heated to a higher temperature and then cooled to the desired temperature to support a faster equilibration. The spikes in the measured mass change are caused by severe pressure variation in the lab and are neglected in the further analysis. The crosses indicate the data points selected as the equilibrium values.

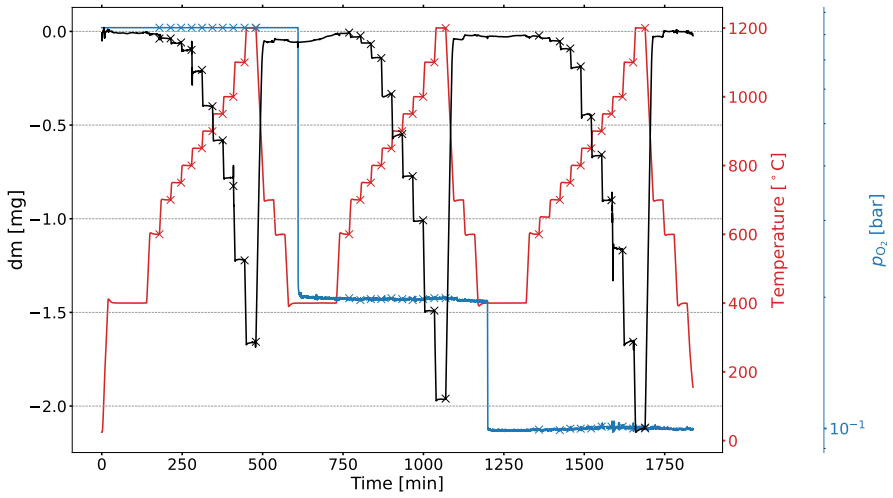

Figure 3 Thermogravimetric scan for thermodynamic analysis of $Ca_{0.9}Sr_{0.1}MnO_{3-\delta}$. A blank measurement was already subtracted from the mass changes shown and a linear drift correction was performed. To reach oxygen partial pressures between $0.83\,\text{bar}$ to $0.1\,\text{bar}$, Ar, N_2 and O_2 were mixed.

The kinetic analysis was performed in a *Netzsch STA 409 CD* thermobalance as described in more detail in the publication. The thermogravimetric scan of $Ca_{0.9}Sr_{0.1}MnO_{3-\delta}$ with a linear drift correction is shown in fig. 5. The oxygen partial pressures were calculated according to the applied gas streams.

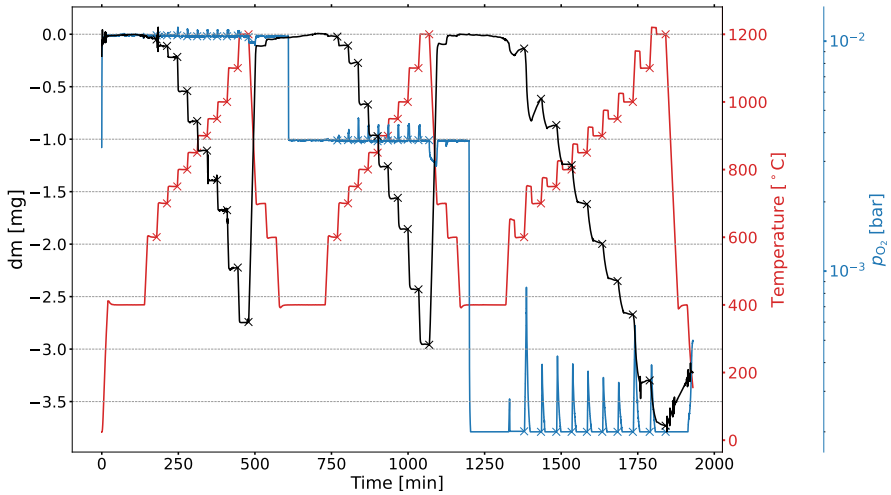

Figure 4 Thermogravimetric scan for thermodynamic analysis of $Ca_{0.9}Sr_{0.1}MnO_{3-\delta}$. A blank measurement was already subtracted from the mass changes shown and a linear drift correction was performed. To reach oxygen partial pressures between 0.01 bar to 1×10^{-4} bar, Ar, N_2 and synthetic air were mixed.

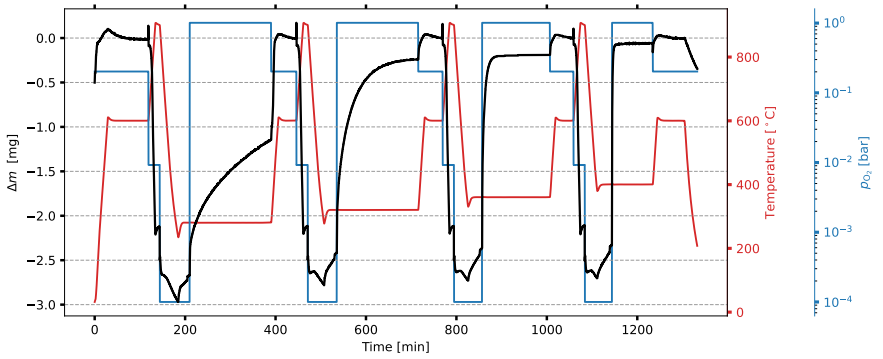

Figure 5 Thermogravimetric scan for kinetic analysis of $Ca_{0.9}Sr_{0.1}MnO_{3-\delta}$. A linear drift correction the mass changes was already performed. Only the oxidation segments were used for further analysis.

3 Thermodynamic analysis

The equilibrium non-stoichiometry δ values against oxygen partial pressure p_{O_2} for different temperatures in K are displayed in fig. 6, 7, 8, 9 and 10. The squares show the experimental equilibirium values and the lines the fit of the applied model.

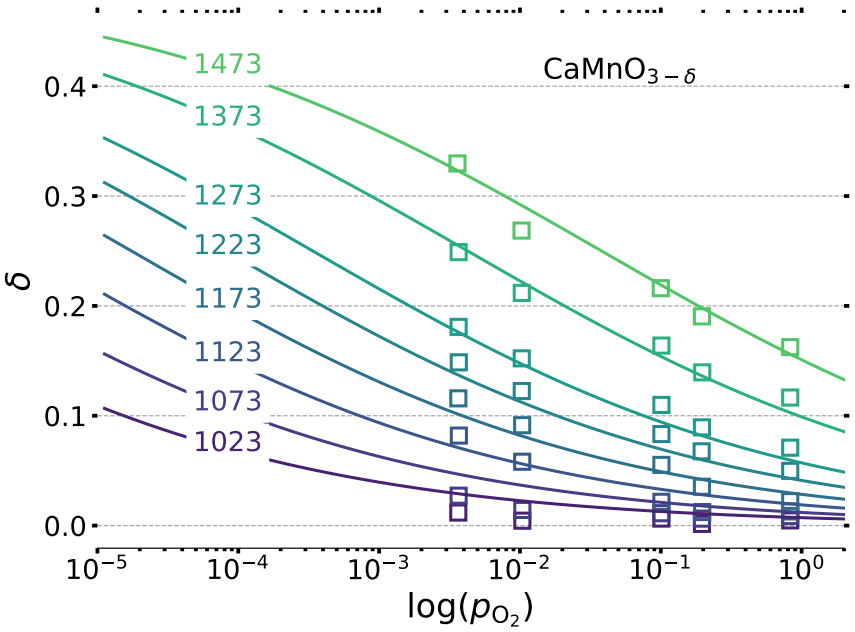

Figure 6 Thermodynamic analysis of $CaMnO_{3-\delta}$.

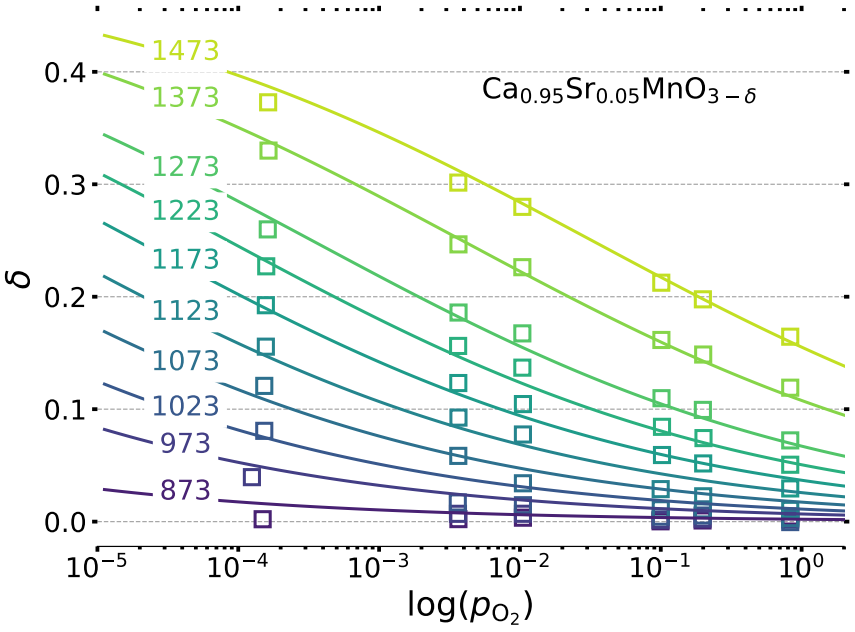

Figure 7 Thermodynamic analysis of $Ca_{0.95}Sr_{0.05}MnO_{3-\delta}$.

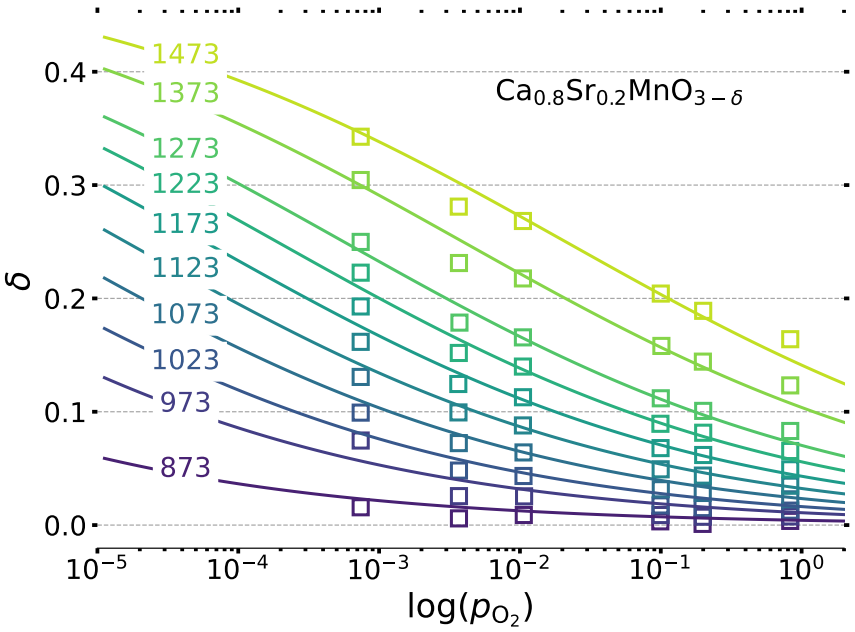

Figure 8 Thermodynamic analysis of $Ca_{0.8}Sr_{0.2}MnO_{3-\delta}$.

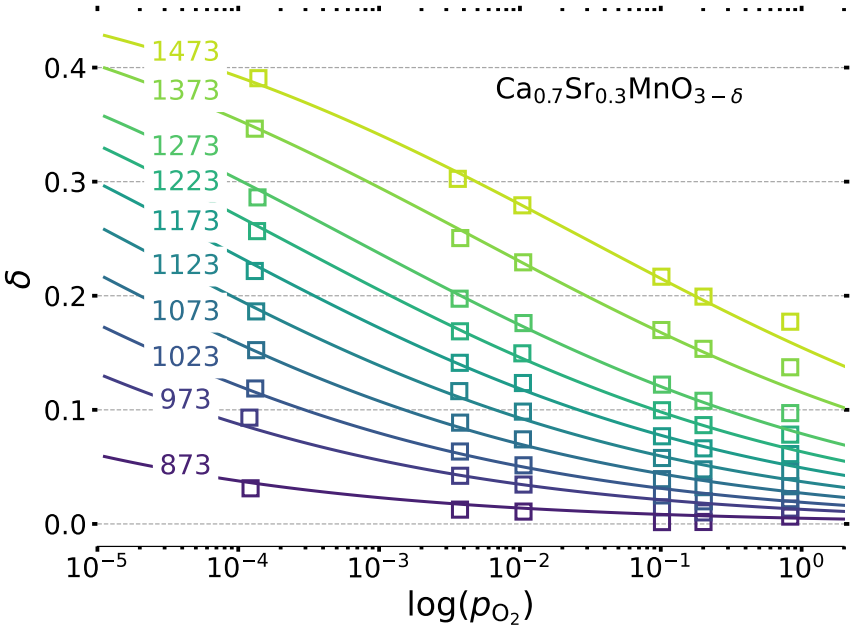

Figure 9 Thermodynamic analysis of $Ca_{0.7}Sr_{0.3}MnO_{3-\delta}$.

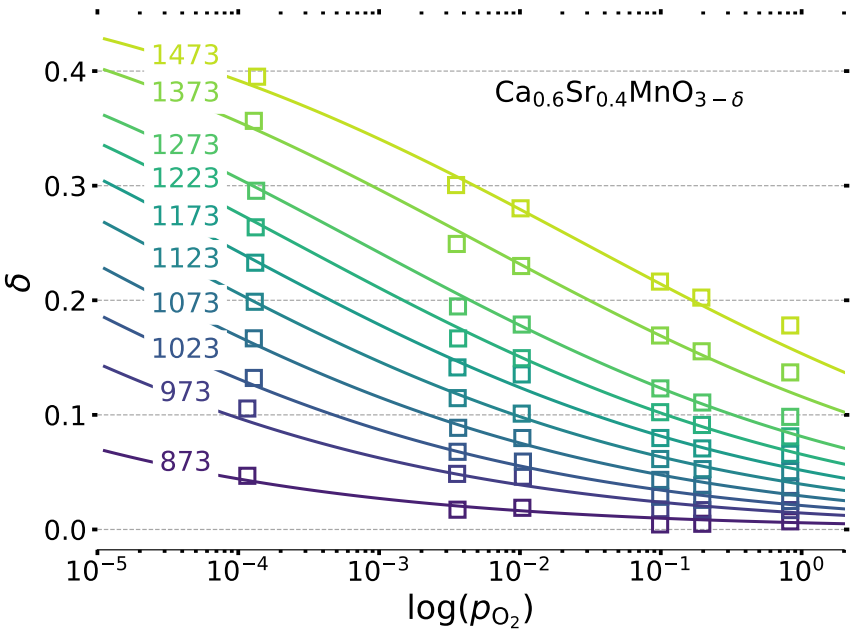

Figure 10 Thermodynamic analysis of $Ca_{0.6}Sr_{0.4}MnO_{3-\delta}$.

4 Kinetic analysis

Table 1 Oxidation kinetic parameters determined by the model fit parameters.

Material	β [-]	k_0 [$s^{-1}(mol\ m^{-3})^{-n}$]
CMO	1.6(7)	4.813×10^9
CS10MO	1.6(5)	3.855×10^9
CS20MO	1.6(5)	3.115×10^{10}
CS30MO	1.6(4)	2.036×10^{10}
CS40MO	2.1(8)	8.150×10^9

References

[1] L. Klaas, M. Pein, P. Mechnich, A. Francke, D. Giasafaki, D. Kriechbaumer, C. Agrafiotis, M. Roeb and C. Sattler, *Physical Chemistry Chemical Physics*, 2022, **24**, 27976–27988.